Research Article

ENERGY EXPLORATION & EXPLOITATION

Energy Exploration & Exploitation
2019, Vol. 37(4) 1253–1267

DOI: 10.1177/0144598719830929
journals.sagepub.com/home/eea
SAGE

Relationship between fault activity and hydrocarbon accumulation in the Baxian Depression, Bohai Bay Basin, China

Kai Zhao[1], Youlu Jiang[1], Jonathan Imber[2], Hongjin Hu[1], Hua Liu[1] and Dexiang Yang[3]

Abstract

Based on the fluorescence microscopic features of fluid inclusions and the combined analysis of the homogenization temperature and burial history modeling, the hydrocarbon charge history was divided into two phases, among which the second phase was the main pool-forming period and took place during the deposition of the Minghuazhen Formation (12–2 Ma). Based on the calculation of the rate of fault displacement and the duration of fault activity, the fault activity characteristics are quantitatively evaluated. The result shows that the average rate of fault displacement during this interval was 6.9 m/Myr, and the duration of fault activity was about 0–6 Myr. Reservoirs formed in the non-hydrocarbon generating strata are overwhelmingly situated adjacent to the faults which have the most rapid displacement rates and longest periods of activity.

Keywords

Fault activity, fluid inclusion, hydrocarbon charge history, hydrocarbon accumulation, Baxian Depression, Bohai Bay Basin

[1]School of Geosciences, China University of Petroleum (East China), Qingdao, China
[2]Department of Earth sciences, University of Durham, Durham, UK
[3]North China Oilfield Branch Company, PetroChina, Renqiu, China

Corresponding author:
Youlu Jiang, School of Geosciences, China University of Petroleum (East China), Qingdao, China.
Email: jiangyoulu@upc.edu.cn

Introduction

Faults are the main channels for vertical migration of hydrocarbons in faulted basins (Hindle, 1997; Jiang et al., 2018). Transport within faults is likely to be important where there is a large stratigraphic separation between the source and reservoir intervals (Jiang et al., 2015). The evaluation of fault activity plays an important role in the study of fault transport, because active and/or critically stressed faults may serve as fluid migration pathways while quiescent faults are more likely to be sealing (Hindle, 1997; Townend and Zoback, 2000). Hence, the rate of fault displacement and the duration of fault activity with the respect to the hydrocarbon charge history are important concepts for studying the effect of fault transport on hydrocarbon migration. Faults may act as important fluid conduits if the period of fault activity coincides with expulsion and secondary migration of hydrocarbons away from the source rock interval (Jiang et al., 2017). Using the effective fault transport as the clue to determine the migration pathways is helpful to reduce exploration risks.

The Baxian Depression is an important oil-rich depression in the Bohai Bay Basin. The hydrocarbons sourced from the Paleogene mudstones were accumulated in multiple stratigraphic levels, and the main oil-bearing series include (in stratigraphic order) the Paleogene Shahejie (E_2s_4, E_2s_3, E_2s_2 and E_2s_1) and Dongying (E_3d) formations, and the Neogene Guantao (Ng) Formation (Zhao et al., 2015). Most of the oils in these strata are distributed near faults. These features indicate that hydrocarbons have migrated vertically and that faults played an important role in the process. Some research has been carried out on the characteristics of fault activity of the Baxian Depression in recent years. Yang et al. (2002) studied the segmentary activity of the boundary fault in the Baxian Depression and analyzed its influence on the structure of the depression. Zhang et al. (2014) studied the fault activity characteristics during the Paleogene and analyzed their influence on the tectonic evolution in the Baxian Depression. Xie et al. (2015) analyzed the influence of fault activity on sand bodies during the deposition of Dongying Formation (E_3d). However, previous studies were limited to the effect of fault activity on sedimentation and structure during the Paleogene, but lacked specific studies on the relationship between fault activity and hydrocarbon accumulation. Large-scale migration of oils occurred during the Neogene and faults served as important fluid migration conducts (Lu et al., 2010). Therefore, the characteristics of fault activity during the Neogene and its relationship with the hydrocarbon filling period are important factors to determine fluid migration pathways.

The objectives of this paper are to: (1) investigate the hydrocarbon filling period through fluid inclusion analysis; (2) evaluate the rate of fault displacement and duration of fault activity; and (3) analyze the effect of fault activity on the hydrocarbon distribution, to provide theoretical guidance for further exploration.

Geological setting

The Baxian Depression is located in the central part of the Jizhong sub-basin and covers an area of approximately 2090 km^2 (Figure 1(a); Liu et al., 2011). Its western part is adjacent to the Niutuozhuang Uplift, its northern and southern parts adjoin the Langgu-Wuqing Depression and Raoyang Depression, respectively, and its eastern part is bounded by the Dacheng Uplift (Figure 1(b)). The Baxian Depression consists of Ertaijie Fault Terrace Buried

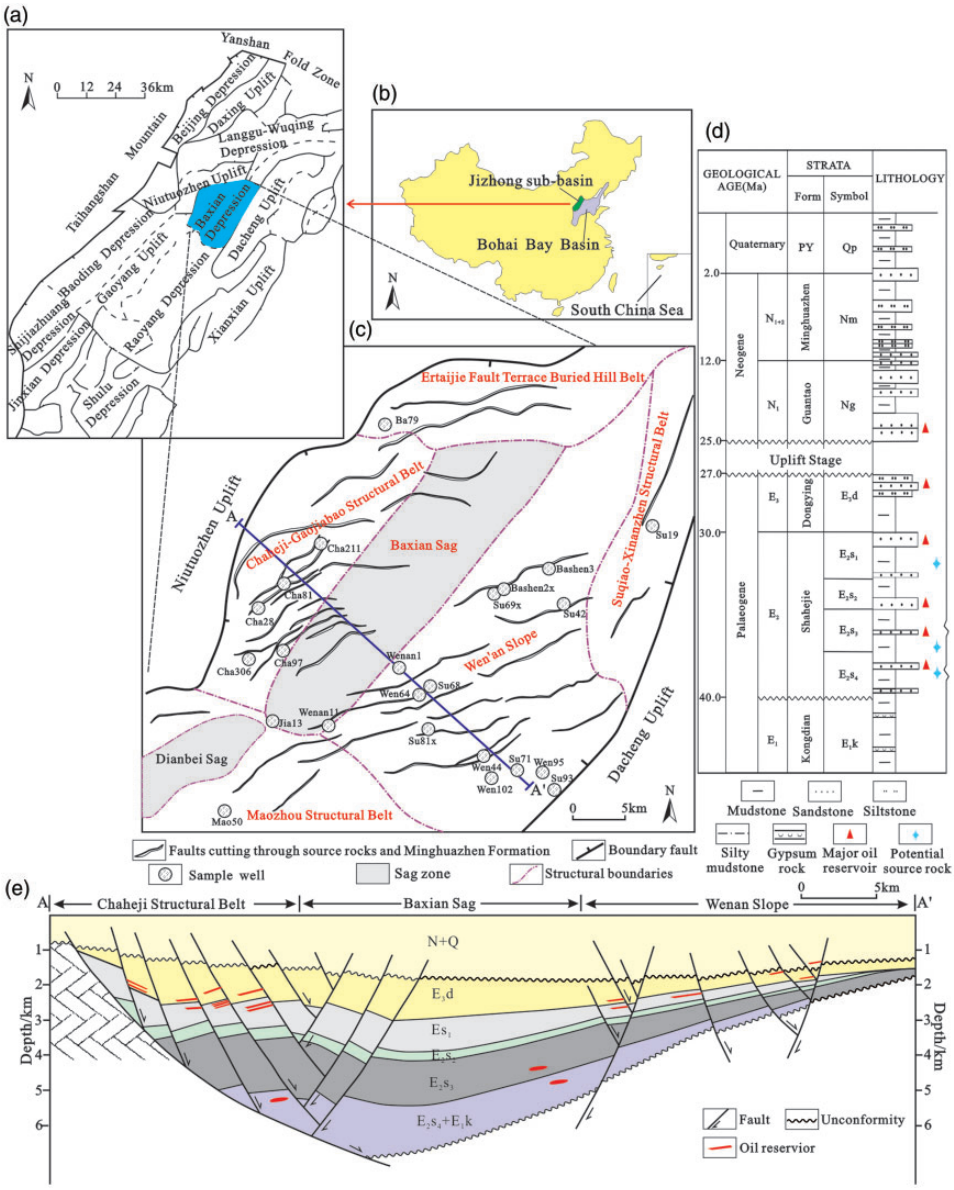

Figure 1. (a) Locations of Bohai Bay Basin and Jizhong sub-basin. (b) Location of Baxian Depression. (c) Main structural units within Baxian Depression, showing the location of sample wells. (d) Stratigraphy of Baxian Depression with possible source rocks and main oil reservoirs. Form: Formation; PY: Pingyuan. (e) Cross section showing structural framework of Baxian Depression. Section location is shown in (c).

Hill Belt, Chaheji-Gaojiabao Structural Belt, Maozhou Structural Belt, Suqiao-Xinanzhen Structural Belt, Wen'an Slope, Baxian Sag, and Dianbei Sag (Figure 1(c); Zhao et al., 2015).

Above the Cenozoic basement, the Baxian Depression can be subdivided into two tectono-stratigraphic levels: a rifting stage (60.5–25 Ma) during the Paleogene and a thermal

subsidence stage (25 Ma to the present) during the Neogene and Quaternary (Zhang et al., 2008). In ascending order, the synrift sediments are represented by the Kongdian (E_1k), Shahejie (E_2s), and Dongying (E_3d) formations (Figure 1(d)). These formations were deposited in fluvial-lacustrine environments. Three hydrogen-rich, oil-prone source rocks have developed in the fourth, third, and the first member of the Shahejie Formation (E_2s_4, E_2s_3, and E_2s_1, respectively), and all of them have been confirmed to be effective source rocks in the Baxian Depression (Huang and Pearson, 1999). The postrift sediments consist of the Guantao (Ng), Minghuazhen (Nm), and Pingyuan (Qp) formations (Figure 1(d)). The Ng Formation is dominated by braided river sandstones whose thickness can reach up to 700 m. The Nm Formation is deposited in a fluvial environment and is dominated by thin interbedded sandstones and mudstones.

Regional uplift in the late Oligocene (27–25 Ma) created the unconformity between the E_3d and Ng formations. After that, the geomorphology was relatively gentle, and the thick sandstones of the Ng Formation covers the whole Baxian Depression (Figure 1(e)).

Sampling and methods

Fluid inclusion petrography

The fluid inclusion petrography studies the fluorescence intensity and color characteristics of hydrocarbon inclusions under ultraviolet (UV) light to identify distinct hydrocarbon charges (Jiang et al., 2016; Lin et al., 2015). In this study, a total of 23 sandstone core samples were collected from 23 wells located in different structural belts within the Baxian Depression (Figure 1(c); Table 1). All samples were made into doubly polished sections of approximately 100 mm, and a Zeiss AXIO Imager D1m digital polarized fluorescence microscope was used in the fluorescence microscopy study.

Fluid inclusion micro-thermometry

Combined with the buried heating history, the homogenization temperatures of the fluid inclusions represent the temperature when the inclusion is formed. Oil inclusions are generally not captured at natural gas saturation, but when restored to a single-phase state it is in saturation condition, so the homogenization temperature of the oil inclusion is generally lower than the trapping temperature, while the homogenization temperature of the associated water inclusions is generally close to the capture temperature. Hence the homogenization temperature of associated brine fluid inclusions associated with hydrocarbon inclusions can represent the temperature when hydrocarbon inclusions were formed (Jiang et al., 2016). In this study, a total of 126 inclusion thin sections were tested for the homogenization temperature by the Linkam THMS600 gas-flow heating/freezing system with a heating rate of 10°C/min.

Burial history modeling method

The burial history was simulated using the basin modeling method (Hakimi and Abdullah, 2015; Makeen et al., 2016). The modeling parameters, including stratigraphic ages, formation depth, erosion thickness, lithology, and boundary conditions (heat flow, paleowater depth and sediment water interface temperature) were all obtained using the Third Resource Evaluation of Baxian Depression.

Table 1. Basic lithological characteristics of the core samples.

Structural belt	Well	Formation	Depth (m)	Lithological characteristics
Ertaijie Belt	Ba 79	E_2s_2	2994.7	Fine sandstone
Baxian Sag	Jia 13	E_2s_3	3687.51	Silestone
	Wenan 11	E_2s_2	3382.1	Fine sandstone
Chaheji-Gaojiabao	Cha 211	E_3d	2949.28	Fine sandstone
Structural Belt	Cha 81	E_2s_1	3274.8	Fine sandstone
	Cha 28	E_3d	2751.5	Fine sandstone
	Cha 306	E_3d	3410.96	Fine sandstone
	Cha 97	E_2s_2	3706.8	Fine sandstone
Maozhou Belt	Mao50	E_2s_3	3378.45	Fine-silestone
SX Structural Belt	Su 19	E_2s_1	2975.3	Fine sandstone
Wen'an Slope	Bashen 3	E_2s_3	3478.01	Fine sandstone
	Bashen 2x	E_2s_1	3325.2	Fine sandstone
	Su 42	E_3d	2368.19	Fine sandstone
	Su 69x	E_2s_3	3858.99	Silestone
	Wenan 1	E_2s_4	4150.92	Fine sandstone
	Su 68	E_2s_3	3536	Fine sandstone
	Wen 64	E_2s_1	2933.5	Fine sandstone
	Su 81x	E_2s_1	2736.37	Fine sandstone
	Wen 44	E_3d	1883.4	Fine sandstone
	Wen 102	Ng	1625.3	medium sandstone
	Su 71	E_2s_2	1971.2	Fine sandstone
	Wen 95	E_2s_1	1596.3	Fine-medium sandstone
	Su 93	E_2s_1	1370.85	Fine-medium sandstone

Ertaijie belt: Ertaijie Fault Terrace Buried Hill Belt; SX Structural Belt: Suqiao-Xinanzhen Structural Belt.

Fault activity quantitative evaluation method

Figure 2(a) shows that the sedimentation rate exceeded the fault throw rate in all periods (Childs et al., 1993). In this case, the footwall sedimentation is controlled by regional subsidence, while the sedimentation of the hanging wall is influenced by both fault activity and subsidence (Lei, 2012). Therefore, we can use the rate of fault displacement, which is defined as the thickness difference between the hanging wall and footwall in unit time, to evaluate the fault activity. The rate of fault displacement is calculated by dividing the thickness difference by the total fault active time, as follows (Figure 2(b))

$$R = \frac{\text{thickness difference between the hanging wall and footwall}}{T} \tag{1}$$

where R represents the rate of fault displacement, with the unit of m/Myr. T represents the total fault active time, with the unit of Myr.

The Neogene (25–2 Ma) was the main hydrocarbon expulsion stage in study area (Liu et al., 2011; Zhao et al., 2015). However, all faults except boundary faults in the study area became inactive during the deposition of Minghuazhen Formation (Nm, 12–2 Ma). Hence, the duration of fault activity during this interval (T_m) is important to evaluate the fault transport. Faults with longer active phase were more favorable for hydrocarbon migration

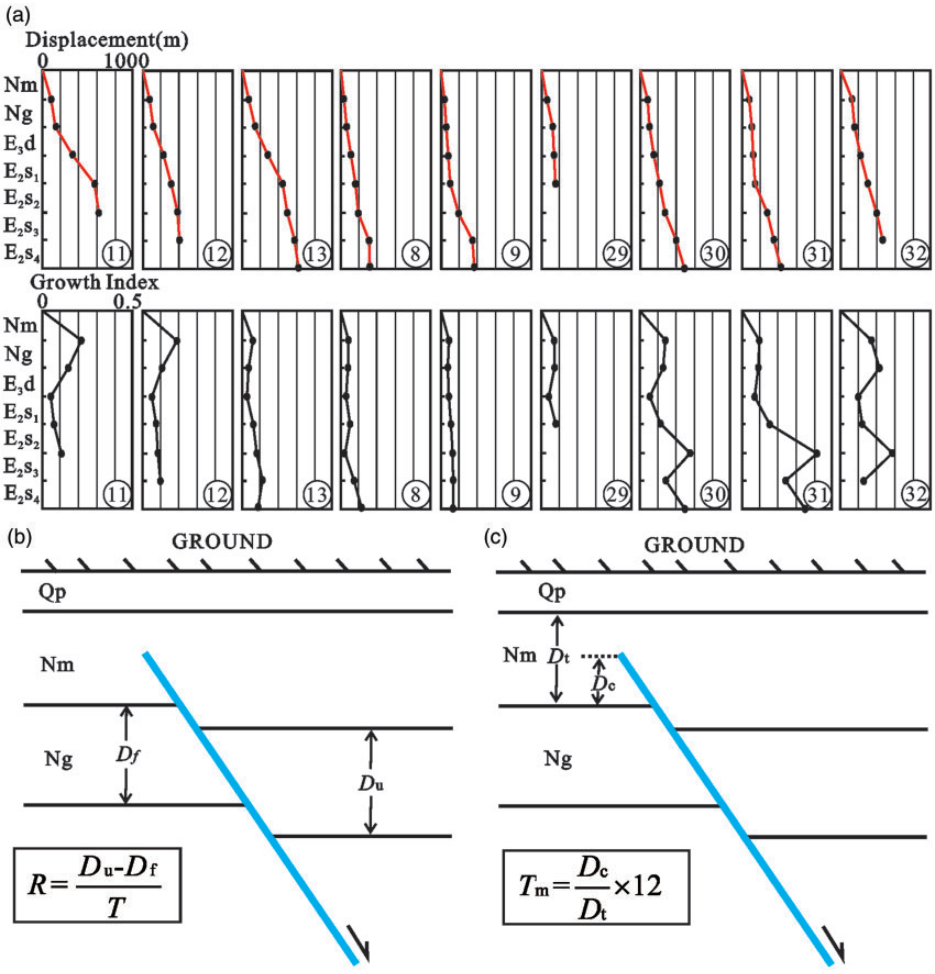

Figure 2. (a) Vertical displacement profiles and growth index of faults on Figure 1(e). Please see Figure 6(a) for fault number. Growth index is defined as (hanging wall thickness – footwall thickness)/footwall thickness (Childs et al., 1993). (b) Calculation of the rate of fault displacement. *Du*: thickness of the hanging wall; *Df*: thickness of the footwall; *T*: total fault active time; *R*: rate of fault displacement. (c) Calculation of the duration of fault activity during the deposition of the Nm. *Dt*: total footwall thickness of the Nm; *Dc*: footwall thickness of the Nm cut by the fault; *Tm*: the duration of fault activity.

(Liu et al., 2016; Shen et al., 2012). The Baxian depression was in the stage of steady subsidence during that time (Zhao et al., 2015). Given the assumption that the footwall sedimentation rate during this interval was relatively stable (Childs et al., 1993), the T_m can be defined as (Figure 2(c))

$$T_m = \frac{\text{footwall thickness of the Nm cut by the fault}}{\text{total footwall thickness of the Nm}} \times 12 \tag{12}$$

where 12 is the deposition time of the Nm, with the unit of Myr.

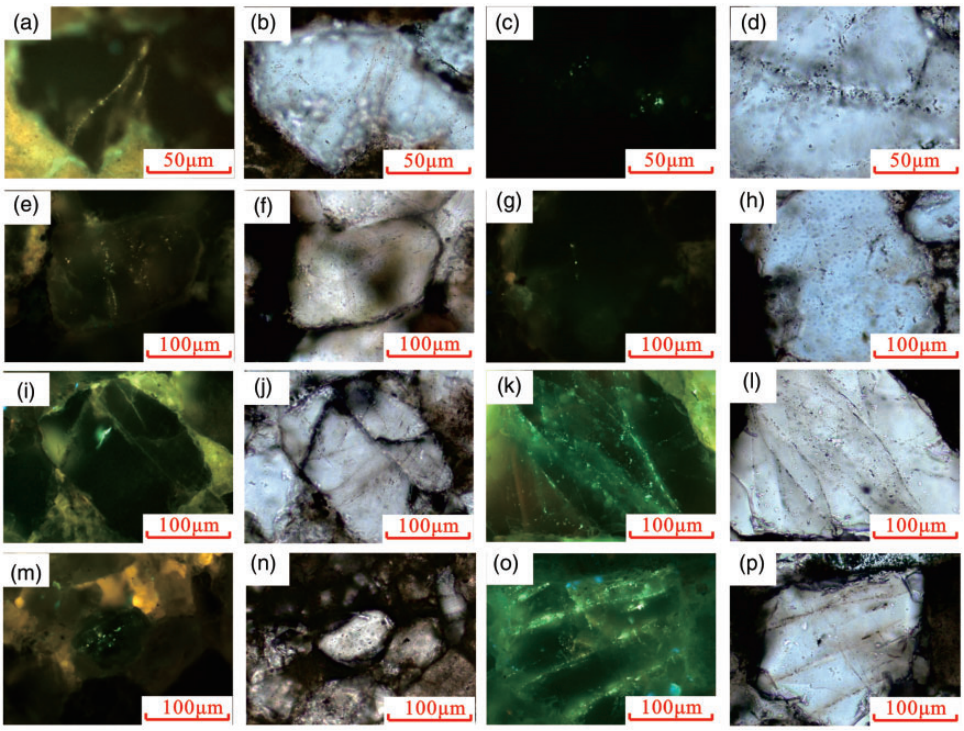

Figure 3. Inclusion photographs under fluorescence and transmitted light of Baxian Depression. (a)–(d) Inclusions occurred in fractures through the quartz grains, Wen'an1, 4150.9 m, E_2s_4 Formation; (e)–(h) inclusions occurred in fractures through the quartz grains, Bashen3, 3478.0 m, E_2s_3 Formation; (i), (j) inclusions occurred in fractures within quartz grains, Su71, 1971.2 m, E_2s_2 Formation; (k), (l) Inclusions occurred in fractures within quartz grains, Wen64, 2933.5 m, E_2s_1 Formation; (m), (n) inclusions occurred in fractures through the quartz grains, Wen44, 1883.4 m, E_3d Formation; (o), (p) inclusions occurred in fractures through the quartz grains, Wen 102, 1625.3 m, Ng Formation.

Results and discussion

Fluorescence microscopy characteristics

Generally speaking, hydrocarbon inclusions forming in the low mature phase of source rock evolution would have a high density, because they have a high content of heavy hydrocarbon and asphaltene. In this case, their fluorescence is mainly brown. As the maturity increases, or the migration and differentiation increases, the crude oil density will decrease. Fluorescence colors of hydrocarbon inclusions captured in this stage are mainly white, yellow or yellow green. Fluorescence colors of hydrocarbon inclusions forming in the mature or highly mature phase are milky blue or blue (Liu et al., 2013).

The hydrocarbon inclusions in the study area can be divided into two categories according to their color characteristics of fluorescence: (1) with low intensity yellow-white fluorescence under UV light and light brown under transmitted light (Figure 3(a), (b), (e), (f)); (2) with high intensity blue-green fluorescence under UV light and almost colorless under transmitted light (Figure 3(c), (d), (g)–(p)). It indicates that there were two stages of

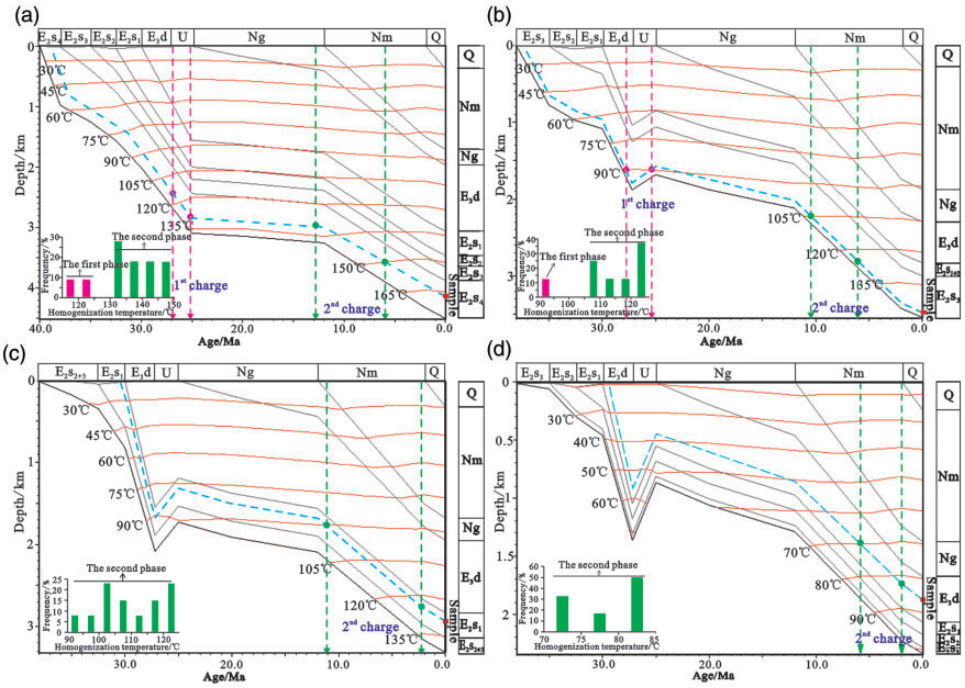

Figure 4. Hydrocarbon charging periods determined by homogenization temperature combined with burial history modelling. a Wen'an1, 4150.9 m, E_2s_4; b Bashen3, 3478.0 m, E_2s_3; c Wen64, 2933.5 m, E_2s_1; d Wen44, 1883.4 m, E_3d. U: the uplift stage.

hydrocarbon filling with different maturity in the study area. The yellow-white fluorescence indicates that hydrocarbon inclusions formed in the relatively low mature phase, while the blue-green fluorescence means that hydrocarbon inclusions formed in the mature phase or highly mature phase (Jiang et al., 2016; Liu et al., 2013).

It can be found that hydrocarbon inclusions formed in the E_2s_4 and E_2s_3 formations always have two fluorescent colors, which shows that there were two phases of hydrocarbon filling within these two formations. The maturity of source rock evolution was low during the first phase of hydrocarbon filling, while the maturity was relatively high during the second one. However, hydrocarbon inclusions formed in the E_2s_1, E_3d and Ng formations always have the blue-green fluorescence only, which indicates that there was only the second phase of hydrocarbon filling in these formations.

Homogenization temperature characteristics and hydrocarbon charging periods

As shown in Figure 4 and Table 2, the time of the first phase of hydrocarbon filling is about 27.8–25.2 Ma (from late E_3d to the late uplift stage), while the time of second phase is about 12–2 Ma (the deposition time of Nm Formation). Besides, the first phase of hydrocarbon filling occurred only in the area within or close to sag zones while the second phase occurred across the whole depression (Figure 5). What is more, there were two hydrocarbon filling periods in the deep E_2s_4 and E_2s_3 Formations, but there was only the second phase occurred in the shallow E_3d and Ng Formations (Table 2), among which the Ng was deposited

Table 2. Homogenization characteristics of fluid inclusions and hydrocarbon charge time in the Baxian Depression.

Well	Formation	Depth (m)	Phase	Homogenization temperature (°C)	Hydrocarbon charge time (Ma)
Wenan 1	E_2s_4	4150.92	I, II	115–125, 130–150	26.8–25.2, 12.8–6
Su 68	E_2s_3	3536	I, II	90–95, 105–130	26.9–25.3, 12.0–4.5
Bashen 3	E_2s_3	3478.01	I, II	90–95, 105–125	27.8–25.5, 10.6–6.2
Su 69x	E_2s_3	3858.99	I, II	85–105, 115–130	26.5–25.5, 11.5–5.2
Mao50	E_2s_3	3378.45	I, II	100–125, 130–140	26.5–25.5, 10.5–5.0
Jia 13	E_2s_3	3687.51	I, II	110–120, 125–140	26.0–25.3, 11.0–4.0
Wenan 11	E_2s_2	3382.1	I, II	100–120, 130–140	26.9–25.3, 11.8–4.5
Cha 97	E_2s_2	3706.8	I, II	90–105, 120–130	26.7–25.5, 11.5–5.5
Ba 79	E_2s_2	2994.7	II	120–135	12.0–6.8
Su 71	E_2s_2	1971.2	II	95–115	10.2–3.4
Cha 81	E_2s_1	3274.8	I, II	80–100, 110–140	26.9–25.0, 10.8–3.0
Bashen 2x	E_2s_1	3325.2	I, II	85–110, 120–140	26.5–25.0, 10.5–3.5
Su 19	E_2s_1	2975.3	II	110–125	12.0–6.5
Wen 64	E_2s_1	2933.5	II	90–125	11.2–2.3
Su 81x	E_2s_1	2736.37	II	95–120	10.8–3.0
Wen 95	E_2s_1	1596.3	II	95–110	10.5–3.5
Su 93	E_2s_1	1370.85	II	75–100	7.5–2.6
Su 42	E_3d	2368.19	II	95–115	6.5–2.7
Wen 44	E_3d	1883.4	II	70–85	5.8–2
Cha 28	E_3d	2751.5	II	110–135	7.0–3.6
Cha 211	E_3d	2949.28	II	105–130	6.2–3.2
Cha 306	E_3d	3410.96	II	85–105	5.5–2.4
Wen 102	Ng	1625.3	II	95–120	6.5–2.5

between the two periods of hydrocarbon charges. Because the number of hydrocarbon inclusions with the second filling phase is much larger than that with the first phase, it can be found that the second filling phase (the deposition time of Nm Formation) was the main pool-forming period.

Cause analysis of the difference in the hydrocarbon charge history

By comparing the pool-forming time in different tectonic belts and different oil-bearing series, it can be seen that the second phase of hydrocarbon filling occurred widely, distributed almost in the whole region and all the oil-layers, while the first phase was mainly distributed close to sag zones and within the deep formations (Table 2). The difference of the hydrocarbon charge history in different parts and different layers is closely related to hydrocarbon generation and expulsion histories.

The source rocks (E_2s_4 and E_2s_3) distributed in the sag zones were in the low mature during the middle and late deposition of E_3d Formation (29–27 Ma; Zeng and Wen, 2011). There was some hydrocarbon generated but only a little expelled. As a result, oils were only accumulated in the strata of source rocks (E_2s_4 and E_2s_3) within or close to deep sag zones at that time. This was the first stage of hydrocarbon generation and expulsion, which corresponds to the first phase of hydrocarbon filling. Then the regional uplift (27–25 Ma)

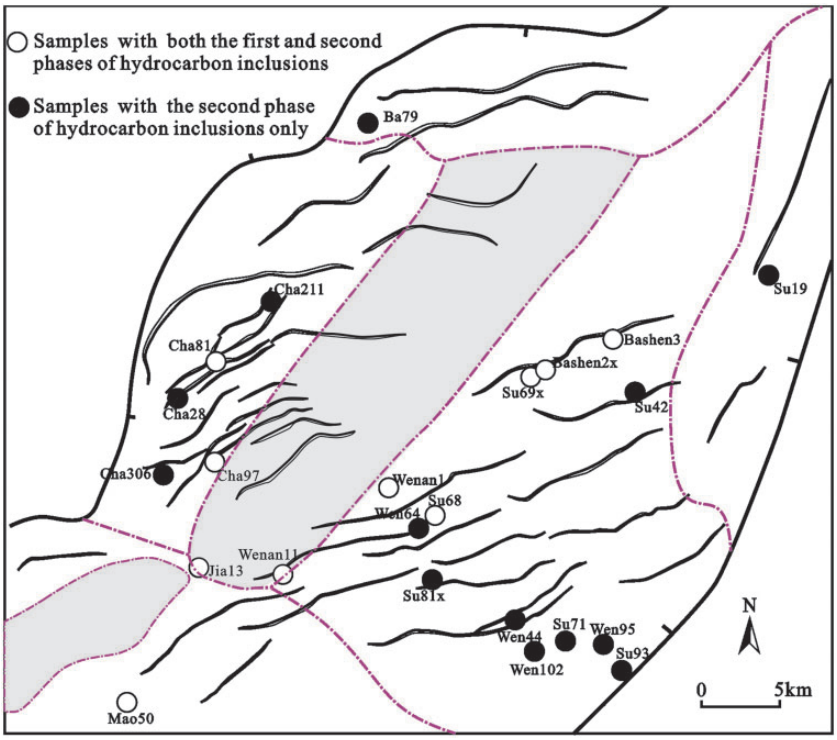

Figure 5. Distribution of hydrocarbon inclusions in different phases of the Baxian Depression.

occurred in the Baxian Depression. The evolution of source rocks stagnated and oils ceased to be generated. Until the late Ng and the early Nm period (13–10 Ma), the burial depth and maturity of source rocks has reached and exceeded the figures before the uplift, and the evolution of source rocks continued. This was the second stage of hydrocarbon generation and expulsion, in which the source rocks were at mature or high maturity stages. Faults acted as the main channel for hydrocarbon migration, and helped the oils migrate to different layers and depths to accumulate during the deposition of Nm Formation. This led to the widespread distribution of the second phase of hydrocarbon filling.

Quantitative evaluation of fault activity

According to equations (1) and (2), the fault activity characteristics in all periods of faults that remain active during the deposition time of Nm Formation are evaluated. These faults might serve as hydrocarbon migration pathways. Using the fault pattern mapped at the base of the Nm, the faults were numbered to facilitate the characterization of their fault activity (Table 3). The average rate of fault displacement was the highest during the deposition of E_2s_4 and E_2s_3. It decreased during the following E_2s_2. Then there was a little rise in the rate during E_2s_1. After that, the figure experienced some deceases until Ng. During the deposition of the Nm, the rate showed an upward trend again and finally reached 6.9 m/Myr. Besides, the average duration of fault activity during the deposition of the Nm was 0–6 Myr.

Table 3. Quantitative evaluation of fault activity in Baxian Depression.

Structural belt	No.	Fault activity rate (m/Myr)							Duration of activity in Nm (Myr)	Fault type
		E_2s_4	E_2s_3	E_2s_2	E_2s_1	E_3d	Ng	Nm		
Ertaijie Belt	1	65.6	53	21.2	25.3	11.9	3.6	4.3	1.2	C
	2	39.5	41	13	27	11.8	1.2	2.3	1.8	C
Baxian Sag	3	35.4	37.1	15	18	9.3	0.5	1.8	0.8	C
	4	31	29.1	10.2	19	11.2	2.6	4.5	1.5	C
	5	39	42.3	19.6	26.1	6.2	3.2	5.4	2.8	B
	6	–	–	12.3	17.4	7.3	2.9	4.2	1.5	C
	7	–	35.6	11.8	14.9	5.9	1.8	2.4	1.9	C
	8	43.2	38.9	15.6	22.1	6.4	2	2.7	0.4	C
	9	25.3	38.4	11.3	25.5	14.6	2.6	3.2	0.9	C
Chaheji-Gaojiabao Structural Belt	10	29.7	42.3	17.6	26.3	12.9	2.2	4.3	1.3	C
	11	–	–	16.5	24.5	14.6	6.9	15.7	5.9	A
	12	–	35.5	14.1	27.5	17.2	5.4	13.4	4.9	A
	13	25.3	38.9	12.9	20	6.4	1.3	4.1	1.3	C
	14	36.2	25.6	10.6	17.4	9.5	3.4	6.4	2.6	B
	15	29.3	34.6	18.5	25.6	15.5	7.1	12.6	3.6	B
	16	34.2	36.6	17.6	27.7	14.9	8.6	13.1	5.5	A
	17	–	32.2	19.2	21.7	9.6	5.9	11.2	4.5	A
	18	–	–	12.8	18.5	7.3	3.2	4.2	1.2	C
Maozhou Structural Belt	19	46.2	41.3	11.1	17.1	5.6	2	4.3	1.5	C
	20	36.1	33.5	14.7	19.2	4.6	1.6	3.8	0.9	C
	21	–	33.1	14.6	17.4	9.7	4	4.1	1.2	C
Suqiao-Xinanzhen	22	32.2	44.4	10.2	11.2	5.6	1.9	2.9	1.9	C
	23	59.3	45.3	11.4	15.5	6.7	2	2.5	1.1	C
Wen'an Slope	24	29.8	33.2	18.6	29.4	10.6	6.3	10.3	3.6	B
	25	26.6	29.6	11.4	27.5	12.4	5.2	8.3	4.1	B
	26	36.2	34.5	9.5	14.4	8.6	5.3	5.6	3.7	B
	27	33.1	32.3	17.2	19.5	4.6	1.3	2.6	1.6	C
	28	48.5	38.7	26.4	29.7	9.4	2.3	4.1	1.5	C
	29	–	–	–	13.2	7.3	3.6	5.3	3.5	B
	30	24.4	32.5	14.3	19.5	12.1	5.6	9.3	4	B
	31	36.9	33.7	20.5	24.6	15.4	4.1	6.9	3.7	B
	32	–	30.3	14.6	19.7	19.4	9.6	12.3	5.7	A
	33	–	–	–	23.9	15.7	10.3	11.2	5.3	A
	34	33.3	29.7	8.6	17.5	13.4	8.7	12.4	4.7	A
	35	–	39.1	21.9	28.4	19.2	10.2	15.5	4.6	A
	36	36.4	37.2	14.4	19.4	8.9	6.3	11.3	5.6	A
Average		36.5	35.4	15	21.5	10.6	4.3	6.9	2.8	

Ertaijie belt: Ertaijie Fault Terrace Buried Hill Belt.

Impact of fault activity on hydrocarbon accumulation

Based on the rate and duration of fault activity during the main hydrocarbon filling period (Nm), the transporting faults are classified into three types (Figure 6(a)): type A (with the rate of fault displacement over 10 m/Myr and duration of activity over 4 Myr), type B (with the rate about 5–10 m/Myr or the duration about 2–4 Myr), and type C (with the rate about

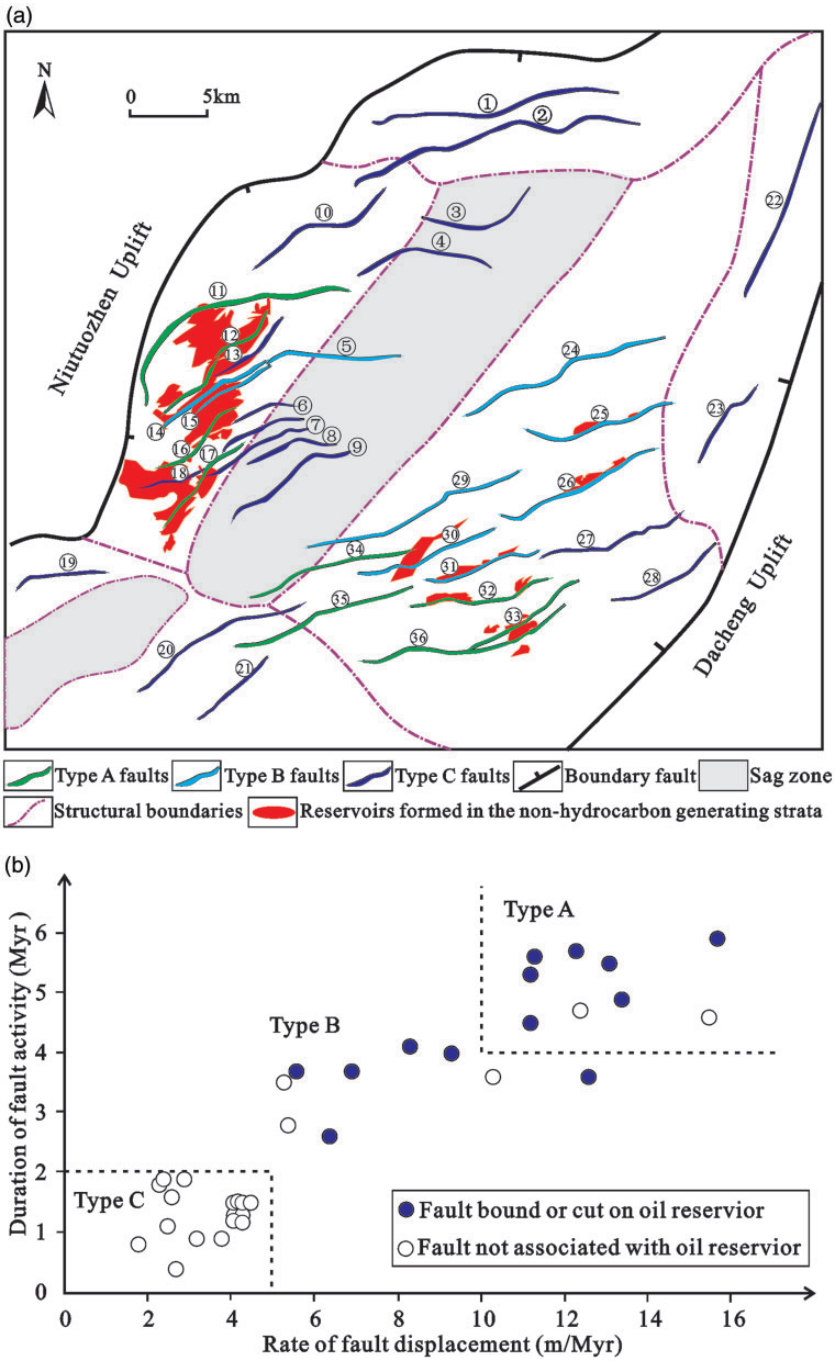

Figure 6. (a) Distributions of fault types and oil reservoirs in the non-hydrocarbon generating strata. (b) Relationship between fault activity and oil reservoirs in the non-hydrocarbon generating strata, with contours of fault types shown (broken lines).

Table 4. The relationship among oil-bearing strata, fault activity, and the thickness of strata above source rocks in different structural belts.

Structural belt	Major oil-bearing series	Average fault activity in Nm		Thickness of the formations (m)		
		Rate (m/Myr)	Duration (Myr)	E_2s_2	E_2s_1	E_3d
Baxian Sag	E_2s_4, E_2s_3	2.2	3.5	320	1000	900
Ertaijie Belt	E_2s_4, E_2s_3	3.3	1.5	300	800	800
SX Structural Belt	E_2s_3, E_2s_1	2.7	1.5	350	800	850
Maozhou Belt	E_2s_3, E_2s_1	4.1	1.2	300	600	600
CG Structural Belt	E_2s_1, E_3d	9.4	3.4	180	400	900
Wen'an Slope	E_2s_1, E_3d, Ng	8.9	4.0	150	350	400

Ertaijie belt: Ertaijie Fault Terrace Buried Hill Belt; SX Structural Belt: Suqiao-Xinanzhen Structural Belt; CG Structural Belt: Chaheji-Gaojiabao Structural Belt.

0–5 m/Myr and the duration about 0–2 Myr). It can be found that reservoirs formed in the non-hydrocarbon generating strata are overwhelmingly situated adjacent to the type A and type B faults which have the most rapid displacement rates and longest periods of activity (Figure 6(b)). Besides, in the regions with more type A and type B faults, the oils always accumulated in shallow layers (above the source rocks), and the responding pool-forming time was relatively later (about 6–2 Ma). From the view of tectonic belts, it is found that Chaheji-Gaojiabao Structural Belt and Wen'an Slope are more favorable for shallow hydrocarbon accumulation, and the traps near type A and type B faults in these two regions shall be the favorable exploration targets of reservoirs in non-hydrocarbon generating strata.

Influencing factors of oil-bearing series

The oil-bearing series of Ertaijie Fault Terrace Buried Hill Belt and Baxian Sag are E_2s_4 and E_2s_3, and the oil-bearing series of the Maozhou Structural Belt and the Suqiao-Xinanzhen Structural Belt are E_2s_3 and E_2s_1. Oils in these areas are accumulated in deep strata near the source rocks. This is because the fault activity in these areas was weak during the hydrocarbon filling period (Table 4), and faults might not serve as effective conducts.

The major oil series in Chaheji-Gaojiabao Structural Belt (E_2s_1 and E_3d) and Wen'an Slope (E_2s_1, E_3d, and Ng) are relatively shallow (Figure 1(e); Table 4). The fault activity in these two areas was stronger than that of the former four regions, and oils tended to migrate to shallow formations through transporting faults. By comparing these two areas, the thickness of the strata above the source rocks (E_2s_2, E_2s_1 and Ed) in Wen'an slope is thinner than that in Chaheji-Gaojiabao Structural Belt. When their vertical migration distances are similar, oils in Wen'an slope are likely to migrate to shallower strata (Table 4), although their fault activity characteristics are similar.

Conclusions

1. The hydrocarbon charge history was divided into two phases. The first phase was from late Dongying (E_3d) to the late uplift stage (27.8–25.2 Ma), while the second phase took place during the deposition of the Minghuazhen Formation (Nm, 12–2 Ma). The second phase was the main pool-forming period. The first phase was mainly distributed near sag

zones and in lower layers, whereas the second phase distributed across the whole depression and mainly in upper layers. The difference of the hydrocarbon charge history is closely related to hydrocarbon generation and expulsion histories.

2. The average rate of fault displacement during the deposition of the Minghuazhen formation (Nm) was 6.9 m/Myr, and the average duration of fault activity during this interval was 0–6 Myr. The transporting faults are classified into three types. Reservoirs formed in the non-hydrocarbon generating strata are overwhelmingly situated adjacent to the type A and type B faults which have the most rapid displacement rates and longest periods of activity during the deposition of the Minghuazhen formation (Nm). With the increase of fault activity and the decrease of formation thickness, oils tend to accumulate in shallower strata.

Acknowledgements

We would like to acknowledge staff of Geological Scientific Research Institute, North China Oilfield Branch Company, for their contribution of data and valuable discussion, which significantly improved the quality of the manuscript.

Declaration of conflicting interests

The author(s) declared no potential conflicts of interest with respect to the research, authorship, and/or publication of this article.

Funding

The author(s) disclosed receipt of the following financial support for the research, authorship, and/or publication of this article: The National Natural Science Foundation of China (Grant No. 41672131) and Fundamental Research Funds for the Central Universities (16CX06045A).

ORCID iD

Kai Zhao http://orcid.org/0000-0002-0166-8358

References

Childs C, Easton SJ, Vendeville BC, et al. (1993) Kinematic analysis of faults in a physical model of growth faulting above a viscous salt analogue. *Journal of Geophysical Research Atmospheres* 114(D14): 1159–1171.

Hakimi MH and Abdullah WH (2015) Thermal maturity history and petroleum generation modelling for the Upper Jurassic Madbi source rocks in the Marib-Shabowah Basin, western Yemen. *Marine and Petroleum Geology* 59: 202–216.

Hindle AD (1997) Petroleum migration pathways and charge concentration: A three-dimensional model. *AAPG Bulletin* 81: 1451–1481.

Huang HP and Pearson JM (1999) Source rock paleoenvironments and controls on the distribution of dibenzothiophenes in lacustrine crude oils, Bohai Bay Basin, eastern China. *Organic. Geochemistry* 30: 1455–1470.

Jiang YL, Fang L, Liu JD, et al. (2016) Hydrocarbon charge history of the Paleogene reservoir in the northern Dongpu Depression, Bohai Bay Basin, China. *Petroleum Science* 13(4): 625–641.

Jiang YL, Liu H, Song GQ, et al. (2017) Differential hydrocarbon enrichment and its main controlling factors in depressions of the Bohai Bay Basin. *Acta Geologica Sinica (English Edition)* 91(5): 1855–1872.

Jiang YL, Liu P, Song GQ, et al. (2015) Late Cenozoic faulting activities and their influence upon hydrocarbon accumulations in the Neogene in Bohai Bay Basin. *Oil & Gas Geology* 36(4): 525–533.

Jiang YL, Zhao K, Liu JD, et al. (2018) A quantitative method for evaluating the transporting capacity of oil-source faults in shallow formation of oil-rich sags. *Acta Geologica Sinica (English Edition)* 92(4): 1678–1679.

Lei BH (2012) Review of methods with quantitative studies of activity intensity of the growth fault. *Advances in Earth Science* 27(9): 947–956.

Lin Z, Zhu X, You F, et al. (2015) Nuclei fluorescence microscopic observation on early embryonic development of mitogynogenetic diploid induced by hydrostatic pressure treatment in olive flounder (*Paralichthys olivaceus*). *Theriogenology* 83(8): 1310–1320.

Liu H, Jiang YL, Xu HQ, et al. (2011) Accumulation mechanisms and modes of Neogene hydrocarbons in Jizhong Depression. *Acta Petrolei Sinica* 32(6): 928–936.

Liu H, Zhao D, Jiang YL, et al. (2016) Hydrocarbon accumulation model for Neogene traps in the Chengdao area, Bohai Bay Basin, China. *Marine and Petroleum Geology* 77: 731–745.

Liu KY, Bourdet J, Zhang B, et al. (2013) Hydrocarbon charge history of the Tazhong Ordovician reservoirs, Tarim Basin as revealed from an integrated fluid inclusion study. *Petroleum Exploration & Development* 40(2): 183–193.

Lu XJ, Liu H, Wang JR, et al. (2010) Petroleum migration system and Neogene petroleum accumulation features in the Baxian Sag, Bohai Bay Basin. *Petroleum Geology &Experiment* 32(3): 258–261.

Makeen YM, Abdullah WH, Pearson MJ, et al. (2016) History of hydrocarbon generation, migration and accumulation in the Fula Sub-basin, Muglad Basin, Sudan: Implications of a 2D basin modeling study. *Marine & Petroleum Geology* 77: 931–941.

Shen P, Zhang SW, Wang YS, et al. (2012) Control of hydrocarbon migration and accumulation by fault and sand body in non-source rocks layers. *Journal of China University of Petroleum* 36(3): 32–37.

Townend J and Zoback MD (2000) How faulting keeps the crust strong. *Geology* 28(5): 399–402.

Xie T, Huang CY, Zhang HW, et al. (2015) Characteristics of syndepositional faults in Baxian Sag and control effects of them on sand bodies in the fault-depression transition period. *Journal of Xi'an Shiyou University (Natural Science)* 30(6): 1–9.

Yang MH, Liu CY, Sun SD, et al. (2002) Extensional tectonic system and its deep-seated setting of Jizhong Basin, China. *Geotectonica et Metallogenia* 26(2): 113–120.

Zeng YT and Wen ZG (2011) Hydrocarbon generation potential of the Es_3 source rocks in Baxian Sag. *Journal of Oil and Gas Technology* 33(8): 31–34.

Zhang WC, Yang DX, Chen YJ, et al. (2008) Sedimentary structural characteristics and hydrocarbon distributed rules of Jizhong Depression. *Acta Geologica Sinica* 82(8): 1103–1112.

Zhang Y, Dai JS, Wang K, et al. (2014) Fault activity features of Baxian Sag in Paleogene in Jizhong Depression. *Journal of Xi'an Shiyou University (Natural Science)* 29(1): 27–33.

Zhao XZ, Liu CJ, Jin FM, et al. (2015) Petroleum genetic types and oil–gas sources of deep reservoirs in Baxian Depression, Northeast China. *Journal of Petroleum Science & Engineering* 134: 105–113.